⟨Superscript⟩

= organic-phase species or organic-phase concentration

Literature Cited

1) Ando, M., S. Emoto, M. Takahashi, T. Kasai and H. Nakayama: Proceeding of 7th Annual Hydrometallurgical Meeting, Vancouver, Aug. 24–25 (1977).
2) Brisk, M. L. and W. J. McManamey: *J. Appl. Chem.*, **19**, 103 (1969).
3) Cook, L. F. W. W. Szmoklank: Proceeding of Int'l. Solv. Extr. Conf., p. 451, The Hague (1971).
4) Davies, J. T. and E. K. Rideal: "Interfacial Phenomena," p. 360, Academic Press, London (1961).
5) Durrani, K., C. Hanson and M. A. Huges: *Metallur. Trans.*, **8B**, 169 (1977).
6) Fordham, S.: *Proc. Royal Soc. London*, **A191**, 1 (1948).
7) Golding, J. A., S. Fouda and V. Saleh: *CIM Special Vol.*, **21**, 277 (1979).
8) Grimm, R. and Z. Kolarik: *J. Inorg. Nucl. Chem.*, **36**, 189 (1974).
9) Komasawa, I., T. Otake and I. Hattori: *J. Chem. Eng. Japan*, **16**, 210 (1983).
10) Komasawa, I., T. Otake and I. Hattori: *J. Chem. Eng. Japan*, **16**, 384 (1983).
11) Komasawa, I., T. Otake and Y. Ogawa: *J. Chem. Eng. Japan*, **17**, 410 (1984).
12) Nirdosh, I. and M. H. I. Baird: *AIChE Symp. Ser.*, **74**, 173 (1971).
13) Preston, J. S.: *Hydrometallurgy*, **9**, 115 (1982).
14) Ritcey, G. M., A. W. Ashbrook and B. H. Lucas: *CIM Bulletin*, Jan., 111 (1975).
15) Shibata, J. and S. Nishimura: *Trans. Japan Inst. Metals*, **23**, 614 (1982).
16) Watanabe, Y., J. Shibata and S. Nishimura: *Tech. Rept. Kansai Univ.*, No. 22, 79 (1981).

THERMODYNAMIC PROPERTIES OF R13 ($CClF_3$), R23 (CHF_3), R152a ($C_2H_4F_2$), AND PROPANE HYDRATES FOR DESALINATION OF SEA WATER

HIRONOBU KUBOTA, KUNIHIKO SHIMIZU, YOSHIYUKI TANAKA, AND TADASHI MAKITA

Department of Chemical Engineering, Kobe University, Kobe 657

Key Words: High Pressure, Phase Equilibrium, Gas Hydrate, Hydrate Formation Condition, Sea Water Desalination, Chlorotrifluoromethane, Trifluoromethane, 1,1-Difluoroethane, Propane

The objective of this investigation was to obtain basic data which are necessary to develop a new hydrate process for desalination of sea water.

Three new hydrating agents, R13 ($CClF_3$), R23 (CHF_3) and R152a ($C_2H_4F_2$), and propane were selected. The pressure-temperature phase diagrams of each agent for pure water and aqueous NaCl solution were determined in the temperature range from 260 to 295 K and pressures up to 4.4 MPa.

Based on the pressure-temperature data obtained, the necessary thermodynamic data, such as hydrate decomposition conditions, invariant points, heat of formation, and hydrate composition were determined.

Introduction

When a gas is present in water at high pressure and at a temperature well above 273.15 K, solid crystals like snow or loose ice in appearance may form. This is called "gas hydrate" and belongs to the category known as clathrates.

In this gas hydrate, water forms a lattice structure and the gas molecules occupy the interstitial vacancies of the lattice without actually taking a lattice position.

Using X-ray techniques, Von Stackelberg and Müller[8,9] determined the X-ray diffraction patterns of gas hydrates. Based upon these X-ray data, Claussen[2] formulated gas hydrate structures into two types, labelled structure I and structure II. **Table 1** gives physical properties of the two structures. As shown in Table 1, each structure has two different-size cavities. The structure formed depends primarily on the size of the guest molecule. For instance, methane and ethane form structure I hydrate and propane and

Received September 26, 1983. Correspondence concerning this article should be addressed to H. Kubota.

Table 1. Structure of Gas Hydrate

	Structure I	Structure II
No. of water molecules per unit cell	46	136
No. of small cavities per unit cell	2	16
No. of large cavities per unit cell	6	8
Diameter of small cavity, 10^{-10} m	7.9	7.82
Diameter of large cavity, 10^{-10} m	8.6	9.46

isobutane form structure II hydrate. In the case of molecules slightly larger than methane and ethane, such as bromine and methyl mercaptane, these molecules occupy only six larger cavities of structure I. These hydrates are called structure I transition hydrates.

Recently, the conditions for hydrate formation have become of great interest in chemical technology, especially in the natural gas industry, desalination of sea water, and purification of waste water.

In this investigation, some thermodynamic property data of R13 ($CClF_3$), R23 (CHF_3), R152a ($C_2H_4F_2$), and propane (C_3H_8) hydrates are determined, in order to develop an economical and energy-saving hydrate process for desalination of sea water.

1. Experimental

The apparatus shown in **Fig. 1** was used to measure the pressures and temperatures at which the hydrate formed or melted. Equilibrium cell A, made of Pyrex glass, was immersed in a constant-temperature bath in which the temperature could be controlled within ± 0.01 K. The pressure was measured by a mercury U-tube manometer and two kinds of strain gage type pressure transducers rated at 1 and 10 MPa, both of which were calibrated against a dead-weight gage. The accuracies of the two transducers were within ± 5 and ± 50 kPa, respectively.

The proper quantity of water or sodium chloride solution, which was used as a model of sea water, was introduced into the equilibrium cell and then the desired amount of hydrating agent was added in a gaseous or liquid state. Agitation of the cell was provided by continuous, vigorous shaking by a mechanical device.

1.1 Determination technique of phase equilibria

To obtain the pressure-temperature phase diagram, the following six kinds of equilibrium conditions are determined. They are schematically shown in **Fig. 2.**

Coexisting Phase	Line
1. Agent-rich liquid + Water-rich liquid + Agent-rich vapor	AE
2. Agent-rich liquid + Agent-rich vapor + Hydrate	AD
3. Water-rich liquid + Agent-rich vapor + Hydrate	AB
4. NaCl solution + Agent-rich vapor + Hydrate	A′B′
5. Water-rich liquid + Agent-rich liquid + Hydrate	AF
6. Agent-rich vapor + Ice + Hydrate	BC

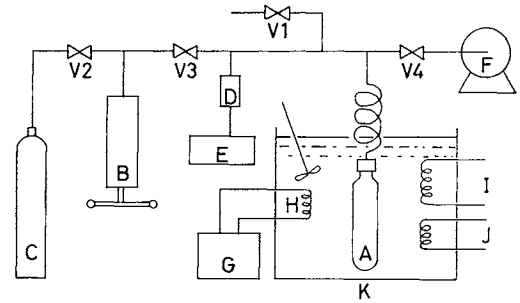

Fig. 1. Schematic diagram of experimental apparatus. A, equilibrium cell; B, screw pump; C, agent gas cylinder; D, pressure transducer; E, digital voltmeter; F, vacuum pump; G, temperature controller; H, heater; I, cooling unit; J, auxiliary heater; V, valves; K, constant-temperature bath.

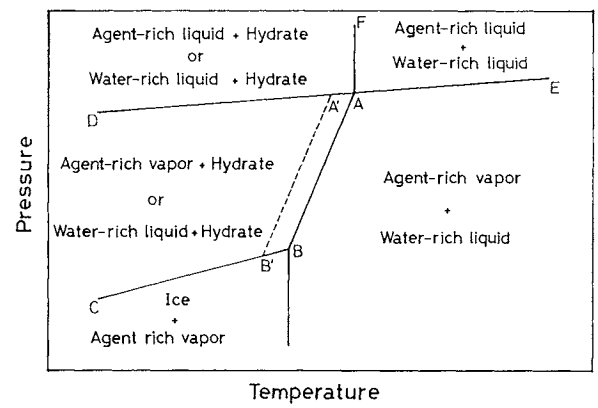

Fig. 2. Schematic phase diagram for hydrate system.

1.1.1 {Agent-rich liquid + Water-rich liquid + Agent-rich vapor}—line AE About one-third of the equilibrium cell was first filled with pure water and then the agent was introduced under such conditions as to form three phases: agent-rich liquid + water-rich liquid + agent-rich vapor, in the equilibrium cell. Temperature-pressure data were taken along this three-phase equilibrium line.

1.1.2 {Agent-rich liquid + Agent rich-vapor + Hydrate}—line AD By cooling the mixture of gaseous agent and liquid water, all water was converted into hydrate. After that, an additional amount of gaseous agent was introduced into the equilibrium cell to ensure the existence of the phases of agent-rich vapor and agent-rich liquid. Temperature was then kept constant at a desired value, which was below the quadruple-point temperature (point A). After that, equilibrium pressures were recorded.

1.1.3 {Water-rich liquid or NaCl solution+Agent-rich vapor+Hydrate}—lines AB and A′B′ The mixture of liquid water or sodium chloride solution and gaseous agent, the pressure of which was below the critical decomposition pressure, was subcooled until the hydrate appeared. The subcooled temperature was usually 5–10 K lower than the equilibrium temperature. Then, the equilibrium cell temperature was raised slowly until the hydrate was just positively present. On this three-phase line, equilibrium temperature and pressure were recorded.

1.1.4 {Water-rich liquid+Agent-rich liquid+Hydrate}—line AF By subcooling the mixture of liquid agent and water near the ice point, the mixture was converted into hydrate to some extent. Then, the temperature was increased slowly until the equilibrium cell temperature was just below the estimated hydrate formation temperature. After that, the equilibrium cell temperature was increased by 0.05 K and the pressure change was observed. If the equilibrium cell temperature was lower than the equilibrium temperature, the pressure was decreased gradually by the formation of hydrate. On the other hand, if the equilibrium cell temperature was higher than the equilibrium temperature, the pressure was increased by the decomposition of hydrate.

1.1.5 {Agent-rich vapor+Ice+Hydrate}—line BC At a temperature above 273 K, all water in the equilibrium cell was converted into hydrate. Then, this mixture was cooled below 273 K and almost all the vapor was pumped out. At a constant temperature below ice point, the mixture was held about 20 hours. Meanwhile, hydrate was decomposed to some extent and the system pressure reached equilibrium pressure. Along this equilibrium line, temperatures and pressures were recorded.

1.2 Materials

The agents R13, R23, and R152a were supplied by Daikin Kogyo Co., Ltd. and their purity was better than 99.9%. The propane was supplied by Seitetsu Kagaku Co., Ltd. The purity was better than 99.5%. Thus impurities would not have affected the experimental results. The water employed was obtained from laboratory distilled stocks and was fractionated once before use in order to remove dissolved gases.

2. Results and Discussion

The hydrating agents intended for use in the hydrate process must have some unique properties. Some of these are high critical decomposition temperature and low critical decomposition pressure, small heat of formation, small depression of hydrate formation temperature due to salt, and large hydrate number.

2.1 Phase diagrams

To determine the pressure-temperarture phase diagrams for R13, R23, R152a, and propane hydrates, equilibrium pressures were obtained over a range of temperature from 260 to 295 K. Some of the data obtained experimentally are listed in **Table 2** and plotted in **Figs. 3** through **5**. There exist two invariant points. The upper one (point A in Fig. 2) is called the critical decomposition point and has four phases in equilibrium. The lower one (point B) is an invariant point with ice. For any fixed salt concentration, these points are shifted to lower temperature and pressures along the lines AD and BC. The temperatures and pressures of the critical decomposition point and invariant point with ice for the pure water and sodium chloride solutions are listed in **Table 4**.

To calculate the thermodynamic data, lines AB, A′B′, AD, AE, and BC are expressed by the following equation:

$$\ln P = a + \frac{b}{T+c} + dT \tag{1}$$

where P is the equilibrium pressure in MPa and T is the equilibrium temperature in K. A least-square fit to our data gives a, b, c, and d for each equation. They are listed in **Table 3** together with the mean deviations between experimental and calculated values. For propane hydrate there exist some experimental data.[4,7,11] Some of these are plotted in Fig. 5 with our data to confirm the validity of our experimental apparatus and technique. Except the data of Wilcox *et al.* at temperature 278.87 K and of Reamer *et al.* at 274.32 K, the present results are found to agree well with those of the other investigators.

No data on R13, R23, and R152a hydrates are available except for the critical decomposition temperature and pressure of R152a (288.45 K, 0.451 MPa).[1]

Obtained results show that among these four agents R23 and R152a have a favorable critical decomposition temperature and small depression of hydrate formation temperature by salt.

2.2 Heat of formation of hydrate

The heats of formation of hydrates from liquid water and gaseous agents are calculated from the slopes of the lines AB on the phase diagrams using the Clausius–Clapeyron equation. The Clausius–Clapeyron equation is written

$$\frac{dP}{dT} = \frac{\Delta H}{T\Delta V} \tag{2}$$

where ΔH is the heat of formation of hydrate and ΔV is the volume change in the hydrate formation reaction.

The following assumptions are made for a binary, three-phase, monovariant system:

1. All phases are pure and do not change in composition.

Table 2. Pressure–temperature data for hydrate system

R13		R23		R152a		Propane	
T [K]	P [MPa]	T [K]	P [MPa]	T [K]	P [MPa]	T [K]	P [MPa]
Line AD, AE		Line AD, AE		Line AD, AE		Line AD, AE	
273.15	1.97	273.15	2.49	273.55	0.271	270.15	0.439
275.05	2.07	276.55	2.72	274.15	0.277	272.05	0.466
277.75	2.21	279.95	2.98	275.05	0.286	272.65	0.475
280.35	2.36	283.15	3.23	278.65	0.323	274.75	0.506
282.15	2.45	284.85	3.37	279.65	0.334	276.55	0.534
284.85	2.62	287.75	3.61	283.05	0.375	277.05	0.542
		289.35	3.77	288.15	0.443	278.15	0.561
Line AB		290.85	3.90	292.15	0.502	279.15	0.579
273.25	0.324	292.05	4.02			279.85	0.590
273.75	0.362	293.55	4.17	Line AB		280.55	0.603
274.65	0.439	295.15	4.33	273.65	0.065	280.65	0.605
276.55	0.660			274.15	0.069	283.65	0.659
277.45	0.806	Line AB		275.35	0.081		
279.25	1.25	273.55	0.353	275.75	0.086	Line AB	
280.85	1.92	275.15	0.426	276.75	0.098	273.25	0.172
281.15	2.14	276.65	0.509	279.05	0.132	273.35	0.174
		278.35	0.623	281.95	0.193	273.55	0.181
Line A′B′ 2.5 wt% NaCl		279.95	0.758	283.55	0.239	273.65	0.187
271.65	0.305	281.65	0.929	285.15	0.296	273.95	0.199
272.75	0.388	283.35	1.14	287.35	0.399	274.15	0.207
273.25	0.432	284.85	1.37			274.65	0.232
274.75	0.598	286.25	1.62	Line A′B′ 2.5 wt% NaCl		274.85	0.239
275.35	0.684	287.75	1.98	272.15	0.060	276.15	0.323
276.65	0.918	289.35	2.48	272.55	0.063	276.75	0.371
278.15	1.32	290.85	3.13	272.85	0.066	277.65	0.455
279.65	2.03	291.75	3.65	274.65	0.082	278.05	0.500
				274.95	0.086	278.15	0.517
Line AF		Line A′B′ 2.0 wt% NaCl		276.95	0.111	278.35	0.542
281.55	3.51	272.55	0.344	279.15	0.149	278.45	0.552
281.55	3.92	274.55	0.435	282.35	0.230		
		276.55	0.555	285.55	0.353	Line A′B′ 2.5 wt% NaCl	
		278.65	0.716	286.65	0.413	270.95	0.138
		280.75	0.921			271.65	0.160
		282.75	1.17	Line A′B′ 3.4 wt% NaCl		271.95	0.172
		284.35	1.43	271.25	0.057	272.15	0.178
		286.45	1.87	272.35	0.065	273.95	0.259
		288.45	2.46	274.15	0.082	276.55	0.471
		290.55	3.44	275.65	0.099		
				276.85	0.116	Line AF	
		Line A′B′ 5.0 wt% NaCl		278.15	0.138	278.45	0.616
		270.35	0.305	279.65	0.168	278.45	0.810
		271.85	0.366	281.35	0.212	278.45	0.921
		273.95	0.469	284.75	0.336		
		275.95	0.595	286.05	0.402		
		278.05	0.769				
		280.15	0.998	Line A′B′ 5.0 wt% NaCl			
		282.35	1.30	270.95	0.059		
		284.05	1.62	271.85	0.066		
		285.95	2.08	273.35	0.081		
		287.75	2.71	275.95	0.112		
		289.15	3.40	279.25	0.175		
				282.95	0.289		
		Line BC		285.15	0.390		
		266.15	0.241				
		268.15	0.265	Line BC			
		269.75	0.285	265.55	0.040		
		271.15	0.304	267.95	0.045		
		272.55	0.384	269.85	0.050		
				270.55	0.052		
		Line AF		271.35	0.055		
		292.35	4.45	272.15	0.057		
				Line AF			
				288.05	0.544		
				288.05	0.823		

Table 3. Coefficients of Eq. (1)

		a	b	c	d	Mean dev. %
R13	Line AD, AE	−5.9154	—	—	2.1449×10^{-2}	0.15
	Line AB	−56.183	−1.1586	−284.05	0.20110	0.41
	Line A′B′ 2.5%	−57.754	−0.63951	−281.84	0.20801	0.10
R23	Line AD, AE	−5.9349	—	—	2.5088×10^{-2}	0.24
	Line BC	−13.713	—	—	4.6180×10^{-2}	0.08
	Line AB	−32.594	−1.0822	−295.49	0.11517	0.27
	Line A′B′ 2.0%	−33.088	−0.67883	−293.60	0.11737	0.19
	Line A′B′ 5.0%	−32.722	−1.1340	−293.36	0.11647	0.22
R152a	Line AD, AE	−10.433	—	—	3.3384×10^{-2}	0.22
	Line BC	−17.678	—	—	5.4426×10^{-2}	0.52
	Line AB	−70.197	−35291	−796.75	—	0.33
	2.5%	−34.488	−8002.3	−524.76	—	0.42
	Line A′B′ 3.4%	−37.571	−9622.0	−548.52	—	0.25
	5.0%	−33.310	−7415.2	−514.19	—	0.45
Propane	Line AD, AE	−8.9752	—	—	3.0185×10^{-2}	0.14
	Line AB	−15.179	−866.98	−337.88	—	0.43
	Line A′B′ 2.5%	−20.922	−1752.8	−363.47	—	0.46

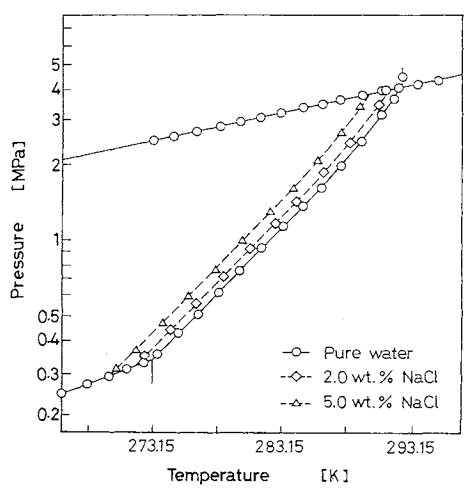

Fig. 3. Experimental phase diagram for R23–water–NaCl system.

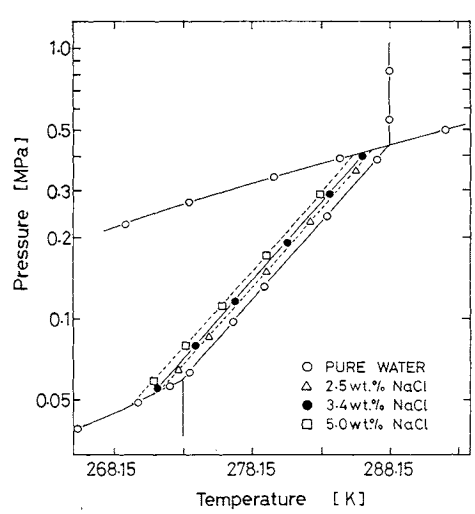

Fig. 4. Experimental phase diagram for R152a–water–NaCl system.

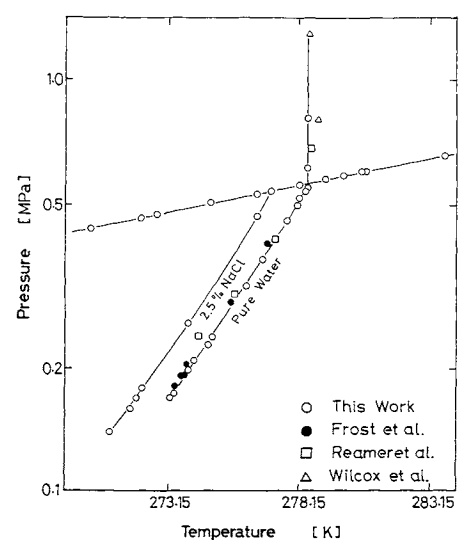

Fig. 5. Experimental phase diagram for propane–water–NaCl system.

2. In the hydrate formation process, the volume of hydrate formed is approximately equal to the volume of water consumed.

Then a simplified expression for Eq. (2) is given by:

$$\Delta H = -RZT^2 \frac{\mathrm{d} \ln P}{\mathrm{d}T} \tag{3}$$

The compressibility factor Z was calculated using the virial equation of state[3] terminated at the third virial coefficient term for R23 and at the second virial coefficient term for R13, R152a and propane. Calculations of ΔH are made at the critical decomposition temperature and 273.15 K. Obtained data for the four agents studied are presented in Table 4.

It is useful to calculate the heat of formation of hydrate on the basis of a unit mass of water solidified

Table 4. Properties of R13, R23, R152a and propane hydrates

		R13	R23	R152a	Propane
Critical decomposition temperature [K]	Pure water	281.50	292.94	288.09	278.54
	2.0% NaCl solution	—	291.15	—	—
	2.5% NaCl solution	280.03	—	286.80	277.18
	3.4% NaCl solution	—	—	286.30	—
	5.0% NaCl solution	—	289.73	285.30	—
Critical decomposition pressure [MPa]	Pure water	2.42	4.04	0.442	0.567
	2.0% NaCl solution	—	3.94	—	—
	2.5% NaCl solution	2.33	—	0.424	0.544
	3.4% NaCl solution	—	—	0.417	—
	5.0% NaCl solution	—	3.80	0.403	—
Hydrate composition					
Method of Pieroen		19.3	7.9	7.6	18.4
Method of Miller and Strong		19.0	7.9	7.6	18.4
Heat of formation of hydrate [kJ/mol-hydrate]					
At critical decomposition temperature		−143.50	−76.44	−85.50	−141.44
At 273.15 K		−125.62	−70.21	−78.68	−123.92
Invariant point with ice					
Temperature [K]		—	272.98	272.94	—
Pressure [MPa]		—	0.331	0.059	—

so that it can be compared with the heat of formation of ice at 273.15 K (6.0 kJ/mol).

At 273.15 K, we obtained the heat of formations as −6.5, −8.9, −10.3, and −6.7 kJ/mol-H_2O for R13, R23, R152a, and propane, respectively.

2.3 Hydrate composition

Because of the experimental difficulty of direct determination of hydrate composition, various indirect methods have been used. In this work, we took the methods of Pieroen[6] and of Miller and Strong.[5]

According to the method of Pieroen, the number of moles of water n associated to the one mole agent may be calculated as follows.

$$n=\frac{\Delta H(T_1-T_2)}{RT_1T_2\ln a_2} \tag{4}$$

$$\text{Agent (gas)}+n\text{H}_2\text{O (liq.)}=\text{Hydrate (line AB)} \tag{5}$$

where ΔH denotes the enthalpy change for Eq. (5) and a_2 is the activity of water, calculated by freezing point depression[10] of pure water with sodium chloride. (T_1-T_2) is the depression of the formation temperature at a constant pressure due to salt. State 1 refers to the conditions in pure water and 2 to those in sodium chloride solution. Hydrate composition n is calculated using equilibrium data shown on lines AB and lines A′B′ (2.0 or 2.5%) in the figures at temperatures from 273.15 K to the critical decomposition temperature of each sodium chloride solution.

The Miller and Strong method gives the following equation:

$$n=-\frac{\ln(f_1/f_2)}{\ln a_2} \tag{6}$$

where f_1 denotes the fugacity of agent in equilibrium with pure water and hydrate and f_2 that with salt solution of known composition and hydrate at the same temperature. The value of n is calculated at temperatures from 273.15 K to the critical decomposition temperature of 2.0 or 2.5% sodium chloride solution by 1 K increments. Values of average hydrate number n obtained from each method are listed in Table 4.

From these values, hydrates for R13, R23, R152a, and propane have structures II, I transition, I transition, and II, respectively.

From the thermodynamic properties obtained above, especially from the standpoint of their formation temperatures and pressures, R152a is considered to be the most suitable among the four agents studied for the hydrate process. R13 and R23 also have fairly high hydrate formation temperatures, but their pressures are rather high for the operation of a large-scale hydrate process.

Conclusion

The temperature-pressure phase diagrams for hydrates of R13, R23, R152a, and propane with pure water or sodium chloride solution were determined at temperatures ranging from 260 to 295 K and pressures up to 4.4 MPa.

Based on the temperature-pressure data obtained, the necessary thermodynamic data, such as heat of formation, hydrate composition, and depression of hydrate formation temperature due to salt, are calculated.

It is thought that the information and data presented may useful in developing a new sea water treatment process by use of gas hydrate.

Acknowledgment

The authors express their appreciation for the financial support given by the Asahi Glass Foundation for Industrial Technology and to N. Hamada for his careful efforts in the measurements.

Nomenclature

a	=	activity	[—]
f	=	fugacity	[MPa]
H	=	enthalpy	[kJ·mol^{-1}]
P	=	pressure	[MPa]
R	=	gas constant	[J·K^{-1}·mol^{-1}]
T	=	temperature	[K]
V	=	volume	[m^3]
Z	=	compressibility factor	[—]

Literature Cited

1) Barduhn, A. J., H. E. Towlson and Y. C. Hu: *A.I.Ch.E. Journal*, **8**, 176 (1962).
2) Claussen, W. F.: *J. Chem. Phys.*, **19**, 259, 1425 (1951).
3) Dymond, J. H. and E. B. Smith: "The Virial Coefficients of Pure Gases and Mixtures," Clarendon Press, Oxford, England (1980).
4) Frost, E. M., Jr. and W. M. Deaton: *The Oil and Gas Journal*, **45**, 170 (1946).
5) Miller, B. and E. R. Strong: *Am. Gas Ass'n. Monthly*, **28**, 63 (1946).
6) Pieroen, A. P.: *Rec. Trav. Chem.*, **74**, 995 (1955).
7) Reamer, H., F. T. Selleck and B. H. Sage: *Petroleum Transactions, AIME*, **195**, 197 (1952).
8) Von Stackelberg, M.: *Naturwiss.*, **36**, 327, 359 (1949).
9) Von Stackelberg, M. and H. R. Müller: *Z. Elektrochem.*, **58**, 25 (1954).
10) Weast, R. C. (Ed.): "Handbook of Chemistry and Physics," 56th ed., CRC Press Inc., Ohio, U.S.A. (1976).
11) Wilcox, W. I., D. B. Carson and D. L. Katz: *Ind. Eng. Chem.*, **33**, 662 (1941).

(A part of this paper was presented at the 15th Autumn Meeting of The Society of Chemical Engineers, Japan, at Kanazawa, October 15, 1981 and at the 23rd High Pressure Conference of Japan at Kyoto, November 18, 1982.)

LONGITUDINAL CONCENTRATION DISTRIBUTION OF DROPLETS IN MULTI-STAGE BUBBLE COLUMNS FOR GAS-LIQUID-LIQUID SYSTEMS

YASUO KATO, TOKIHIRO KAGO AND SHIGEHARU MOROOKA

Department of Applied Chemistry, Kyushu University, Fukuoka 812

Key Words: Chemical Reactor, Three Phase, Bubble Column, Droplet, Holdup, Dispersion, Slip Velocity, Multiphase Flow

The longitudinal concentration distribution of droplets dispersed in multi-stage bubble columns was analyzed by the one-dimensional dispersion model with an effective slip velocity of droplets. The variables of the model—mean gas holdup, longitudinal dispersion coefficient of droplet phase and droplet concentration at the top of the column in 4- and 8-stage bubble columns of 6.6 and 12.2 cm i.d.—were measured and correlated. The effective slip velocity was determined by comparing observed mean droplet concentrations with theoretical ones and was correlated in an experimental equation. The concentration distributions of droplets calculated with the above parameters are in good agreement with the observed ones. Mean droplet diameter was also correlated as a function of gas velocity, total liquid velocity and free area of horizontal baffle plates.

Introduction

A bubble column containing a dispersed organic liquid phase is useful as an efficient contactor for gas-liquid-liquid systems (G-L-L systems). The droplet phase may be a liquid catalyst, an extracting solvent, and so on. Though many studies have been reported on the droplet size in agitated vessels,[15] information on the droplets in bubble columns is quite limited.[2,3,17]

Yoshida and Yamada[17] measured the average diameter of kerosene droplets dispersed in bubble columns which were operated batchwise with respect to liquid. Hatate *et al.*[2] measured gas holdup, longitudinal dispersion coefficient of droplet phase, effective slip velocity between droplet and continuous liquid, and longitudinal concentration distribution of droplets in bubble columns. Hatate *et al.*[3] also correlated the average diameter of droplets as a function of gas velocity, interfacial tension and bubble column

Received December 1, 1983. Correspondence concerning this article should be addressed to S. Morooka.